Experimental Assessment of Aluminum Witness Sheets as Human Skin Surrogates for Vulnerability and Lethality Studies

G. Pageau[1], and A. Bouamoul[2]

[1]*Promaxis Systems, 2385 St. Laurent, Ottawa, ON, K1G 6C3, Canada,*
gilles.pageau@ecn.forces.gc.ca
[2]*Defence Research and Development Canada – Valcartier, Department of National Defence, 2459 de la Bravoure Rd., Québec City, Québec G3J 1X5, Canada.*

Abstract. Many ballistic test standards for vulnerability and lethality studies of armour and anti-armour systems specify the use of aluminum witness sheets to assess the potential for body injury or incapacitation from fragment impacts. The aluminium grades, tempers, and thicknesses vary across different standards. Al 2024-T3 sheets, typically 0.5 mm in thickness, are primarily used when performing V_{50} ballistic limit tests to assess the complete perforation of armours as per the Protection criterion. Following a literature review, only limited evidence was found to correlate to some degree the relevance of aluminum witness sheets as a suitable surrogate for assessing human skin and soft tissue injuries during ballistic and explosive munitions tests. The test and analyses conducted at Defence Research and Development Canada (DRDC) as a part of this study showed that none of the three aluminum alloy sheets tested (i.e., 0.5 mm 2024-T3, 0.4 mm 1060-O and 0.5 mm 1000-O) provided a good match to the human skin lower bound perforation threshold over the broad range of relevant projectile sectional densities. From the review and analysis of previous work studies, a 0.55 mm Al 1100-H12 showed better agreement, but further experimental characterisation would be required, especially for the smaller and lower-density fragments. To account for the effect of skin thickness and density, the regression analyses of the V_{50} data were performed as a function of the dimensionless ratio of the skin areal density over the projectile sectional density. The analysis results for the polystyrene foam used in the body armour mannequin demonstrated that the predicted V_{50} response for 50 mm-thick polystyrene foam would fit within the skin perforation targeted response corridor, making such a witness material worth further characterising experimentally.

1. BACKGROUND: THE USE OF WITNESS SHEETS AND PACKS IN BALLISTIC TESTS

The first reported uses of witness sheets in ballistic test applications were documented in a 1948 study by the Battelle Memorial Institute [1] on laminated composite armour tests, followed by a study of Victory Plastics in 1953 [2] on experimental personal armour materials. The witness material specified was Duralumin 24ST, now referred to as Al 2024-T3, with a thickness of 0.51 mm. In 1959, Mascianica [3] published at the Watertown Arsenal Laboratory (WAL) his monograph on ballistic testing methodologies, where he was the first to introduce the concept of Army, Navy and Protection ballistic limits (V_{50}), which is the velocity for which there is a 50% probability for complete penetration of the armour, calculated from the statistical analysis of the binary outcome obtained, i.e., partial or complete penetration. The specific degree of target damage required to consider the projectile as having successfully perforated the armour sample differs under the Army, Navy, and Protection criteria. Under the Protection Criterion (PC), an impact is defined as a complete penetration if the projectile or back spall fragments from the target have sufficient energy to perforate the witness plate mounted securely and parallel to at a given distance (typically 15 cm) behind the target with the presence of a crack or a hole permitting the passage of light. Any impact rebounding from the armour plate, remaining embedded in the target, or passing through the target with insufficient energy to create a crack without visible light passing through is a partial penetration. For the Army Criterion (AC), a complete penetration occurs when a projectile or fragment has penetrated or caused enough damage to permit the passage of light through a hole or a crack in the armour, including cases when the projectile remains embedded in the armour with the front of the fragment or nose of the projectile being visible from the rear of the armour sample. Impacts that create bulges without cracks, allowing light to pass through, are considered partial penetrations. The effects of potentially lethal behind-armour debris from back spalling or scabbing of the armour are not considered with the Army criterion, which is then less severe than the Protection Criterion. For the Navy Criterion (NC), which is the most severe of the three, a complete penetration occurs when the entire projectile or a significant portion passes entirely through the armour, with all other impacts classified as partial penetrations. No witness plates are employed for tests using the Army and Navy criterion, as a significant portion of the projectile must pass through the armour to obtain a complete penetration.

https://doi.org/10.52202/081621-0055

Figure 1 illustrates a case where the projectile became embedded in the armour target, ejecting the plug and piercing the aluminium sheet. The use of aluminium witness sheets has been adopted in many standards (Table 1, Refs. 4-12), including the assessment of potential injuries from the front spall of hard body armour [11].

Figure 1: Embedded projectile in an armour plate: front (left), rear (centre), and witness sheet (right).

NATO AEP-2920 [13] is not listed in Table 1 because it does not specify the material type and thickness of the witness sheet. Since the aluminum material grades, temper, and thickness differ between standards, this will likely lead to diverging injury risk assessment and lethality/vulnerability outcomes for the same armour and ammunition conditions which would prevent making reliable performance comparisons, especially for lower areal density armour targets with V_{50} ballistic resistance of the same order as the aluminum witness sheet. The 0.5 mm-thick aluminum witness plate has long been assumed to be a surrogate or simulant for human skin in assessing the potential of soft tissue penetrating injuries. TOP-2-2-710 [5] refers to the study by F. James [14] in 1969 on standardising witness materials for ballistic testing, but no copy of the study report was found. From the literature review, only four relevant studies [15-18] were found that correlated the relative ballistic resistance to projectile penetration between thin aluminum witness sheets and human skin. Lee [15] and Hsiao [16] in Taiwan have explored the validity of using aluminum 1100-H14 in thicknesses ranging from 0.5 to 0.65 mm for assessing the safety and wounding capability of air guns. Jakobsen [17] in Norway conducted tests with a 4.5 mm steel sphere and found that the 0.5 mm aluminum 1050-H4 witness sheet was suitable as a skin simulant for the abdomen and back areas but not adequately simulating other body areas (thorax, thigh, buttocks), raising the need to explore aluminum sheets with lower ballistic resistance for making conservative injury assessments.

Metallic Witness Packs (WPs) also utilise aluminum sheets in a spaced array configuration for behind-armour debris assessment and live-fire arena testing of fragmenting munitions. The WP sandwich structure, with aluminum plates and low-density expanded polystyrene foam layers [19], enables the recovery of fragments between the plates, making them also more rigid when scaled to large dimensions. They have been used extensively during the development of Personal Defence Weapons (calibre 4.6mm and 5.7mm) for assessing the relative incapacitation overmatch capability when defeating the NATO's CRISAT target (20 aramid layers + 1.6-mm titanium plate, [20]), simulating a typical body armour at a range of 100 m. WPs have the advantage of sustaining multiple fragment impacts and maintaining their performance regardless of temperature, which is important for outdoor trials. According to NATO STANAG 4164 [12], the first layer of the standard WP consists of a 1 mm thick 1050-H14 aluminum. G. James [18] found that such a WP configuration was not suitable for assessing soft tissue injuries from secondary fragments (e.g., soil ejecta) during buried Improvised Explosive Device (IED) tests, as only denting of the first aluminum layer occurred without any perforation. By comparing the relative ballistic perforation resistance of the 1-mm aluminum sheet to the one of human skin, he demonstrated that for lower sectional density fragments (i.e., small diameter and low specific gravity), the soft tissue injury severity gets significantly underestimated, such that using WPs for collateral damage and safety assessments should be made with caution. Expanded polystyrene foam with a mass density of 15 kg/m^3 was found to be too fragile and incapable of resisting blast loading. NATO AEP-97 [10] also specifies the use of witness plate target arrays with the first layer made of 0.5-mm Al 2024-T4 for the standard armour V_{50} tests used in the development and acceptance testing of armour systems.

Table 1. Aluminium witness sheet grades and thicknesses used in test standards.

Organisations & Standards:	VPAM PM [4]	FFI [17] TNO Witness Pack [32]	TOP 2-2-710 [5]	MIL-STD-662F MIL-STD-3038 NIJ 0108.01 NATO AEP-55&97 US DOD ESAPI	STANAG 4164 [12] DRDC WP	Taiwan [15, 16]	DRDC Current Study	
Alloys / Properties	2017-T4	1050-H4	5052-H36	2024-T3/T4 (24ST Dural)	1100-H14	1100-H12	1060-O	1000-O
Thickness (mm)	0.5	0.5 FFI 1.0 TNO	0.4	0.5	1.0	0.55	0.4	0.5
Density (kg/m^3)	2790	2710	2680	2780	2710	2710	2780	2710
YS (MPa)	276	110	240	270-280	117	92	24	26
TS (MPa)	427	103	280	400-430	124	110	70	90
Elongation (%)	20	8	9	10 to 15	5	10	30	32

YS: Yield Strength; TS: Tensile Strength; FFI: Swedish Defence Agency; TNO: Dutch Defence Agency

2. BALLISTIC TESTS: MATERIALS AND METHODS

The test series to assess the ballistic limit (V_{50}) were conducted on three aluminum grades: the standard 0.5 mm 2024-T3, a 0.4 mm (26 gauge) 1060-O (annealed/soft) flashing roll, and a 0.5 mm (24 gauge) Al-1000-O cold-rolled (see Table 1). The aluminum 1100 and 1060 compositions are identical to the 1050 alloy, as they are part of the commercially pure family (1xxx series). A total of 168 shots were performed for the nine (9) test series. The Al 2024 and Al 1100 witness plates measured 30.5 cm x 30.5 cm, while the Al 1060-O samples had a width of 35.6 cm and were cut into lengths of 45.7 cm and flattened from their roll form. The experimental setup for the test firings is shown in Figure 2. The aluminum sheets were tested at room temperature in the air-backed condition and were secured to a rigid frame with four clamps placed around their edges. The Al 1060-O and Al 1000-O were also tested (series B4 and C2 in Table 2) in conjunction with a 50 mm-thick extruded (XPS) foam backing (Owens Corning Foamular NGX-600), similar to the expanded polystyrene foam (EPS) used in US Army body armour foam mannequins [21]. Aluminum 2024-T3 and 1060-O sheets were tested against 2.5 mm (0.065 g) and 6.35 mm (1.045 g) chrome alloy steel spheres (grade G20, 60 HRC) and the 5.4 mm fragment simulating projectile (un-skirted FSP, 1.105 g [13]). The projectiles were selected to cover a range of shapes and sectional densities (1.3 to 4.8 g/cm²). Aluminum 1000-O was only tested against the 6.35 mm ball. The projectiles were launched with a single-stage gas gun, designed to have interchangeable smooth-bore barrels of various inner diameters that matched the projectile's dimensions, eliminating the need for using sabots. The pressure tank can be filled with helium, nitrogen, or dry air at pressures up to 41 MPa from high-pressure cylinders, allowing velocities of up to 750 m/s ± 5 m/s with the 5.4 mm FSP. The V_{50} tests were conducted under standard conditions of AEP-2920 [13], using the up-and-down firing method as outlined in Annex H to determine the number of shots required to obtain reliable V_{50} estimates. The required velocities were attained by adjusting the gas pressure.

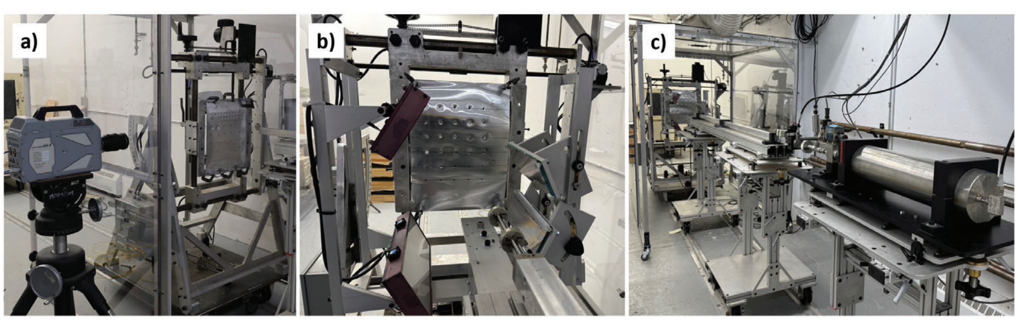

Figure 2: DRDC gas-gun test setup with the high-speed camera (a), mirrors (b), and launch tube (c).

https://doi.org/10.52202/081621-0055

The plate perforation assessment was performed after each impact using the Army criterion. A shot spacing of 10 calibres was used; however, for the softer Aluminium alloys (1060-O and 1000-O), the spacing was increased to prevent overlapping of damage, as shown in Figure 3. For the tests with the 2.5- and 6.35-mm spheres, the target was positioned at a distance of 30.5 cm from the gun barrel, while for the tests with the 5.4 mm FSP, the muzzle-to-target distance was increased to 45.7 cm to allow for using a double mirror system [22] to measure the projectile yaw. The impact velocity of all three projectiles and the yaw angle for the 5.4 mm FSPs were measured using a high-speed video camera (Photron FASTCAM SA-Z) with a rate of 15,000 frames per second. The Yaw HSV image analysis software [23] was used to compute the FSP total yaw angle at 15.2 cm from the witness sheet from the two orthogonal views of the FSP in flight. For the FSP tests, a gun extension was used to help limit the initial yaw, which remained highly variable, ranging from 2° to 10°. More shots were fired to obtain a sufficient number of partial penetrations with yaw angles lower than 5°. The instability of the 5.4 mm FSP is likely caused by firing from a smooth-bore gas gun, which is necessary for achieving low-impact velocities not achievable with powder guns having rifled barrels.

Table 2. Projectile types, aluminium grades, and thicknesses tested with V_{50} ballistic limit (±95% CI) results. (S: series, #: number of shots, T: thickness, AD: areal density, SD: sectional density, AC/NC: Army/Navy criteria).

S #	Projectile	Mass (g)	Aluminum grade & temper	T (mm)	Density (g/cm³)	AD (g/cm²)	SD (g/cm²)	V_{50-AC} V_{50-NC} (m/s)	ΔV_{50}* (%)
A1 18	2.5mm ball	0.065	2024-T3	0.5	2.78	0.139	1.32	178.7±3.4 209.6±14.7	+28.0 +50.1
A2 22	6.35mm ball	1.045	2024-T3	0.5	2.78	0.139	3.30	117.4±1.6	+16.5
A3 14	5.4mm FSP	1.105	2024-T3	0.5	2.78	0.139	4.83	77.9 (0° yaw)	-11.6
B1 17	2.5mm ball	0.065	1060-O	0.4	2.78	0.111	1.32	138.2±0.1 148.8±7.7	-0.9 +6.7
B2 17	6.35mm ball	1.045	1060-O	0.4	2.78	0.111	3.30	67.1±0.1	-33.4
B3 22	5.4mm FSP	1.105	1060-O	0.4	2.78	0.111	4.83	52.9 (0° yaw)	-40.0
B4 17	6.35mm ball	1.045	1060-O + XPS foam	0.4	2.78	0.111	3.30	72.2±0.4	-28.3
C1 25	6.35mm ball	1.045	1000-O	0.5	2.71	0.136	3.30	110.5±2.1	+9.7
C2 16	6.35mm ball	1.045	1000-O + XPS foam	0.5	2.71	0.136	3.30	112.4±4.4	+11.5

* Relative to human skin Probit V_{50} equation from James [18] for adult thigh spherical/pointed fragments

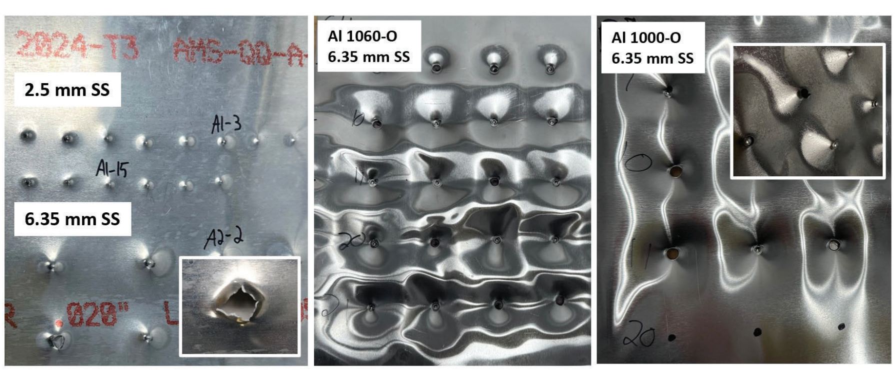

Figure 3: Post-impact damages on witness sheets: 2024-T3 (left), 1060-O (centre), 1000-O (right).

3. BALLISTIC TESTS: RESULTS AND ANALYSIS

The V_{50} results were obtained by performing a logistic regression analysis of the fair shots for each test series using the V_{50} Assist software [23] and the Probit link function with 95% confidence intervals (Table 2). For test series A3 and B3, logistic regressions were performed using two independent variables (velocity and yaw) and with the penetration status as the dependent variable. The probability plot obtained using the Test Science application [24] is shown in Figure 4 (left), with similar results presented in a different format using the V_{50} Assist Yawgit function [23]. For the tests with 2.5 mm spheres (A1, B1), gradual cracking failures of the aluminium sheet occurred at velocities near V_{50}, leading to different interpretations of the penetration outcome (partial or complete) depending on whether the Army or Navy criterion is applied. The analyses were then performed by applying both the Army and the Navy criteria (red colour in Table 2) to allow comparison with previous studies. The Navy criterion is often used since it is less prone to misinterpretations. For the tests with the 6.35 mm sphere and the 5.4 mm FSP, failure by cracking did not occur; instead, the plates failed due to a combination of petalling and plugging (Figure 3), with no perforation issue observed between the Army and Navy criteria. For the V_{50} values computed using the Army criterion, the width of the 95% confidence intervals is less than 4 m/s due to the very narrow zones of mixed results, making the V_{50} values reliable even though only one repeat was performed for each test series. The human skin probit V_{50}s were computed using James' [18] perforation equation, with coefficients for intact adult thigh skin versus spherical and pointed fragments. The difference between the human skin V_{50} values (139.6 m/s for the 2.5 mm sphere, 100.8 m/s for the 6.35 mm sphere, and 88.1 m/s for the 5.4 mm FSP) and those obtained for the tested configurations is provided in the last column of Table 2. It can be observed that the perforation resistance of 0.5 mm Al 2024-T3 is 28% higher for the 2.5 mm sphere and 16.5% for the 6.35 mm sphere, while being 11.6% lower for the 5.4 mm FSP. A reverse trend is observed, with the 0.4 mm Al 1060-O being 25% easier to perforate on average than human skin. The 0.5 mm Al 1000-O alloy provides a closer match to human skin, with an 11.5% higher V_{50} for the 6.35 mm sphere. The foam backing used in test series B4 and C2 did not significantly increase the V_{50s} obtained compared to the no-foam condition.

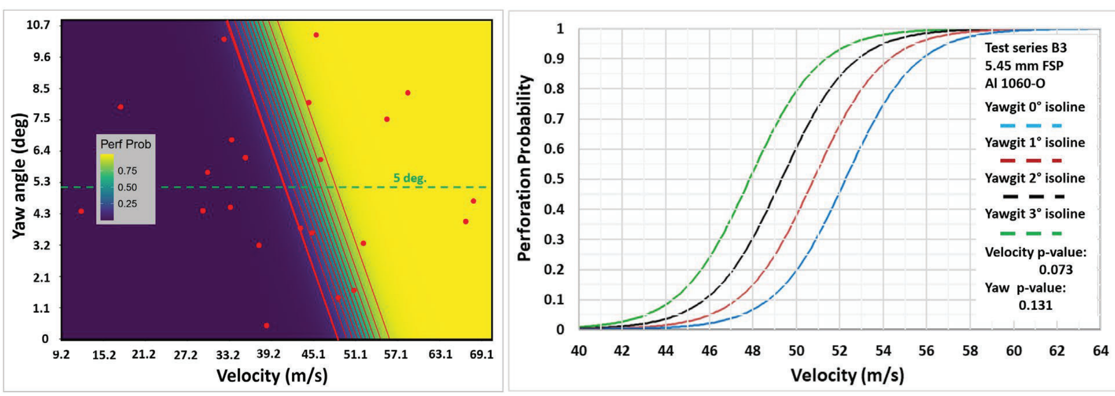

Figure 4: Logistic regression probability plots for the B3 test series: Test-Science (left), and Yawgit (right).

4. COMPARISON WITH PREVIOUS STUDIES AND TARGETED RESPONSE SELECTED

The logistic regression curves (Probit) obtained for the 2.5 mm sphere versus the 0.5 mm Al 2024-T3 witness sheet are compared in Figure 5 with the experimental one provided by Hudgins [25] for goat skin impacted by 2.38 mm (0.055 g) steel spheres. The skin perforation equations by James [18] are presented in Figure 5, along with the predicted V_{50} value for goat skin against the 2.38 mm sphere. The Probit curves obtained for the 0.5 mm Al 2024-T3 are shown to provide significantly higher ballistic resistance for such a low sectional density (SD) projectile compared to the experimental data, highlighting the risk of underestimating skin perforation injury risks from these smaller fragments when using such a witness sheet specified in most standards.

https://doi.org/10.52202/081621-0055

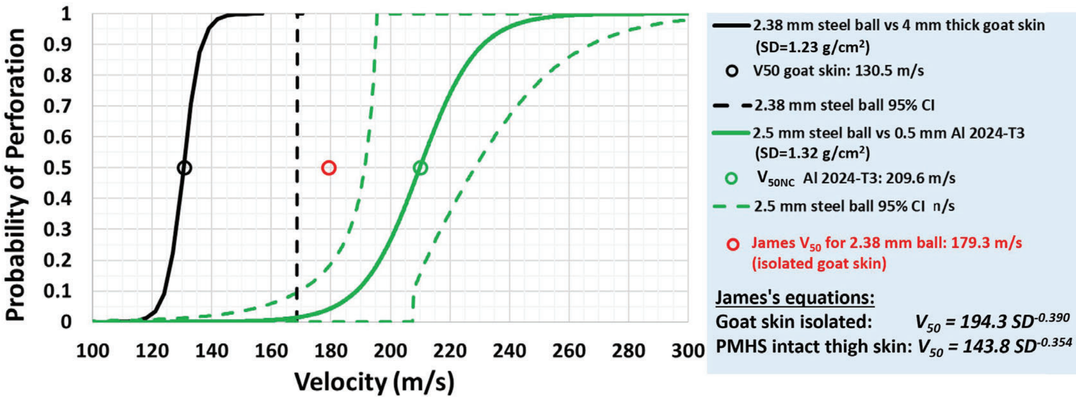

Figure 5: Probit of 2024-T3 vs. 2.5 mm ball (green curves) and goat skin vs. 2.38 mm ball (black curves, [29]) compared to James's equation prediction (red dot) for goat skin vs. 2.38 mm ball.

For better assessing the suitability of the various aluminum witness materials for estimating the risk of skin injury, relevant data from previous studies with 1-mm thick aluminum witness sheets [26-28] and recently published data on Post Mortem Human Subjects (PMHS) [29] and porcine skins [30] were analysed taking into account the effect of target thickness (T) of the aluminum sheet and PMHS/animal skins by following the approach of Cunniff [31] where theV_{50} of armour materials is correlated to the dimensionless areal density ratio: ***CR = AD/SD***, and where ***AD = ρ·T*** is the target Areal Density and ***SD = Mp/Ap*** is the projectile Sectional Density with **Mp**: projectile mass, **Ap**: cross-sectional area, **T**: target thickness, and **ρ**: mass density. The skin perforation model of Hudgins [29] employs a similar parameter (**P**), **where *P = 2/CR***. In addition to accounting for target thickness, this correlation is more intuitive, as a target thickness of zero (**CR=0**) results in a null ballistic limit (**V_{50}=0**), thereby preventing a vertical asymptote at low values of **SD** and **P**. The results are displayed in Figure 6 using a logarithmic scale on the horizontal axis to better visualise the V_{50} response for smaller fragments. When skin thickness data were unavailable, a value of 2 mm was used based on the mean thickness reported in the literature.

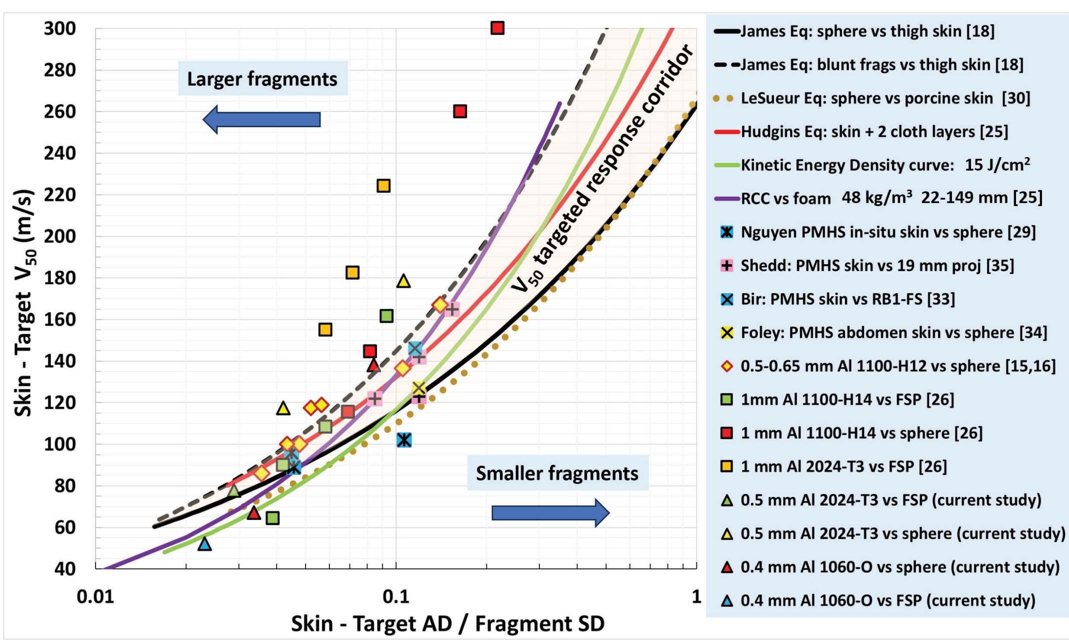

Figure 6: V_{50} vs. AD/SD for aluminum, PMHS/animal data and polystyrene foam.

In Figure 6, the skin perforation equation from James [18] for the thigh area, with the coefficients for spheres used to provide the lower bound for the smaller and lower-density fragments. The upper bound of the proposed targeted V_{50} response corridor was computed using James' equation with the coefficients for blunt fragments. When considering skin thickness, the perforation resistance curves from Hudgins [25] and LeSueur [30] follow the lower bound from James's model for spheres. Kinetic Energy Density (KED) has also been proposed as a threshold for skin perforation, with reported values varying considerably between 5 and 25 J/cm^2 [32]. A KED value of 15 J/cm^2 provides a curve fitting midway between the lower and upper bounds defined by James's equation; however, it underpredicts V_{50}s for the larger and higher-density fragments. Using larger KED threshold values (e.g., 20 J/cm^2) would shift the curve upward, making human vulnerability assessments less conservative. The data points from Bir (anterior on rib, [33]), Foley [34], and Shedd [35] for non-lethal projectiles on PMHS and animal skins are also shown to be consistent, as they lie within the targeted response corridor. It can be observed that the ballistic resistance of the 1-mm 2024-T3 and 1-mm 1050-H14 aluminum sheets used as the first layer in witness packs falls well outside the corridor with much higher V_{50}s, making them unsuitable for fragment hazard studies, as the injury risks to personnel would be underestimated. The Hudgins perforation equation [25], with coefficients for skin covered by two cloth layers, is shown to give a good average fit between the proposed targeted response corridor, which can be used to evaluate the suitability of candidate surrogate skin materials.

Regression analyses of the data points in Figure 6 for the various aluminum grades and thicknesses, as well as the data of LeSueur for porcine skin, were performed using Curve Expert Professional software [36] and a two-parameter power function. The data of the body armour mannequin [21], designed for live-fire testing, were also curved fitted (light blue curve in Fig. 6) for the three thicknesses (22 mm, 73 mm, 149 mm) of extruded polystyrene (EPS, 48 kg/m^3 density) foam tested which was tested against the four standard US Right Circular Cylinder (RCC) fragments. The EPS foam response can be seen to fall mainly within the targeted response biofidelity corridor. The curve fit equations, which were performed as a function of AD/SD, were then re-computed as a function of the reciprocal of the projectile sectional density, referred to as the form factor **F = 1/SD**. The calculations were performed using the original AD values for each case except for the polystyrene foam, where the predicted curve was computed for the more standard panel thickness (50 mm) and density (35 kg/m^3). The curves obtained are shown in Figure 7, along with the 95% confidence and 95% prediction bands from the regression analysis of LeSueur's data, which encompass the previously defined response corridor (red curves).

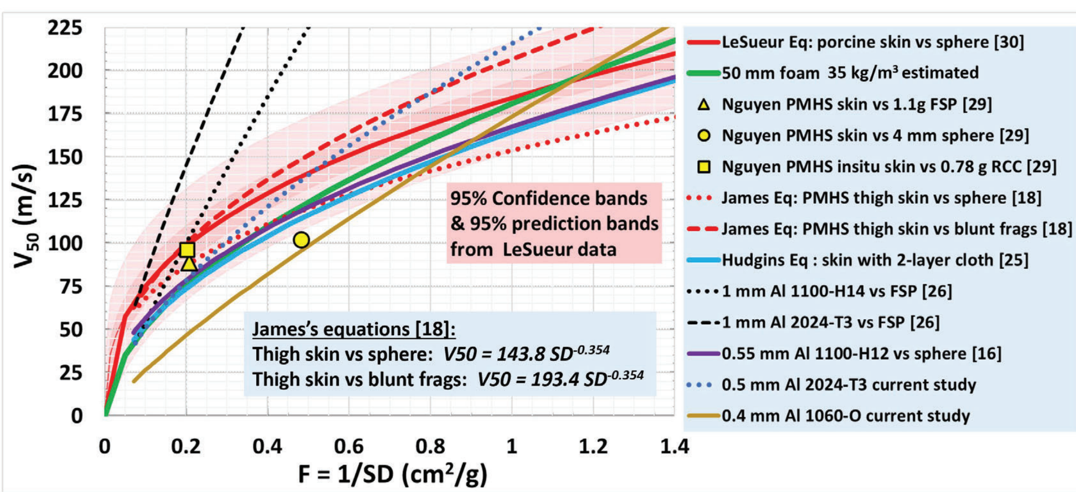

Figure 7: V_{50} versus 1/SD for aluminum, PMHS/animal data, and 50 mm foam (35 kg/m^3).

In Table 3, the areal density of XPS foam panels (50 mm thick, 35 kg/m^3 density), more easily available than EPS foam, is shown to lie between the AD for the 0.5 mm aluminum sheet and the one for human skin (2.5 mm thick).

https://doi.org/10.52202/081621-0055

Table 3. Aluminium and EPS/XPS foam material properties compared to human skin.

Material	Thickness (cm)	Density (g/cm³)	AD (g/cm²)	Strength
Aluminum alloys	0.050	2.7	0.135	24-280 MPa (tensile)
XPS Foam 35 kg/m³	5	0.035	0.175	0.41 MPa (compressive)
EPS Foam 14 kg/m³	5	0.014	0.070	0.07 MPa (compressive)
Human skin	0.25	1.1	0.275	17-28 MPa (tensile)

The overall trends in Figure 7 are similar to those observed in Figure 6, with the 1 mm thick aluminum sheets in both grades exhibiting significantly greater perforation resistance than animal and human skin for form factor (F) values beyond 0.2 cm^2/g. The linear horizontal scale used in Figure 7 explains the changes in the shape of the V_{50} response curves relative to those presented in Figure 6. Some minor curve shifting also occurred, as not all data points in Figure 6 from previous studies were for the same skin thicknesses. The 0.5mm Al 2024-T3 response (dotted blue line) remains above the lower band based on James's equation (dotted red line) for the full range of form factor while exceeding the James upper band for F values beyond 0.8 cm^2/g. The 0.4 mm Al 1060-O is shown to have insufficient ballistic resistance for F values under 0.8 cm^2/g. The regression line from Hsiao's data [16] for the 0.55 mm 1100-H12 aluminum aligns with the lower corridor and could be considered more suitable than the standard 0.5 mm Al 2024-T3. It would be worthwhile to explore the response of thinner sheets (e.g., 0.45 and 0.5 mm) of the same alloy over a broader range of projectile sectional densities and shapes (i.e., RCC, FSP) to validate whether a better match could be obtained for F values beyond 0.45 cm²/g. The recent data for PMHS skin from Nguyen [32] fall within the response corridor, except for the 4 mm sphere, which falls below it.

The predicted response (green line) for the 50 mm-thick polystyrene foam is situated in the central area of the proposed corridor, indicating that such a foam could be used as a replacement for aluminum sheets for ballistic limit tests of armour materials using the Protection criterion. The significantly higher strength of the 35 kg/m³ XPS foam compared to the 14 kg/m³ EPS foam tested by James [18] suggests that this material could be suitable for live fire explosive trials involving combined blast and fragment loadings. Its performance is anticipated to be comparable to that of the ARL body armour mannequin, which is constructed with a slightly denser foam grade (48 kg/m³). The foam panel would provide the advantage of being able to recover the embedded fragments from overmatch shots and measure the Depth of Penetration (DoP) of the fragments, which is impossible with witness sheets, where only a binary outcome is obtained. Figure 8 compares the DoP response of PMHS (red curve, [18]) to that of EPS foam (black curve, 48 kg/m^3 density [24]) for impacts with 16-grain RCC (1.037 g, 5.5 mm) surrogate fragments. The DOP response curves of polystyrene foam and PMHS soft tissues are observed to differ less than anticipated. The foam material exhibits a smoother response, characterised by deeper cavities, particularly at low velocities, with no identifiable threshold velocity required to initiate penetration. The foam's greater compliance would allow for improved velocity discrimination from the DoP measurements.

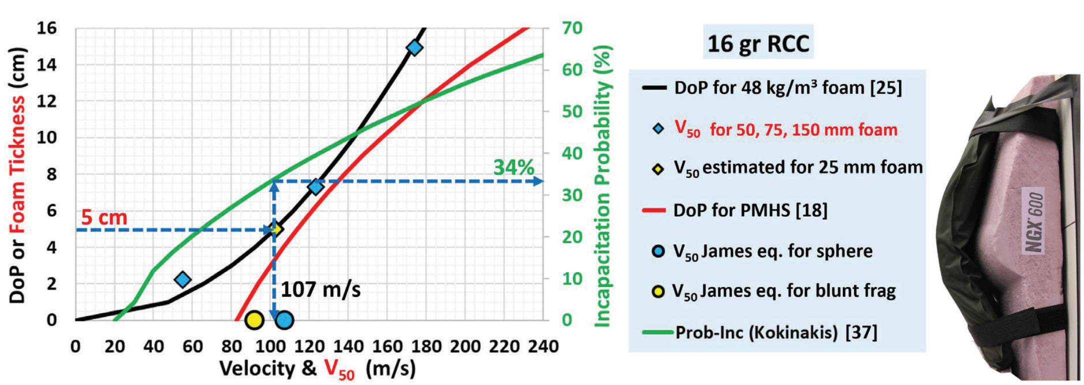

Figure 8: DoP response of XPS foam vs PMHS with V_{50} values and incapacitation probability for the 16-gr RCC (left); an example of a shaped XPS foam backing for armour testing (right).

The corresponding incapacitation probabilities were also computed using the Kokinakis-Sperrazza incapacitation model [37], employing coefficients for the entire body in a defensive role. In Figure 8, a DoP of 5 cm within the 48 kg/m^3 polystyrene foam is shown to correspond to a probability of incapacitation of 34% using the impact velocity (107 m/s) derived from the foam's DoP response curve (black line).

5. SUMMARY AND CONCLUSIONS

The ballistic resistance of standard 2024-T3 aluminum alloy, along with two potential substitute aluminum witness sheets (0.4 mm Al 1060-O and 0.5 mm Al 1000-O), with lower mechanical strength due to their annealed condition, was evaluated against three projectiles with varying sectional densities and shapes (2.5 mm and 6.35 mm steel spheres, and 5.4 mm FSP). Ballistic data from relevant studies on aluminum alloys used in metallic witness packs (1 mm Al 2024-T3 and Al 1100-H14), as well as those from the ARL body armour foam mannequin, were also included for comparison. The V_{50} data for the various skin and material configurations were correlated against the Cunniff dimensionless areal density parameter. The data from previous studies using non-lethal projectiles demonstrated greater consistency when analysed using this approach, which is physically more relevant since it accounts for skin thickness and for which V50 = 0 when AD = 0. The data analyses conducted also confirmed that the ballistic resistance of a 1-mm-thick aluminium used in witness packs is significantly too high, leading to non-conservative injury assessments during vulnerability-lethality trials. Although the V_{50} of 0.5 mm 2024-T3 aluminum is substantially lower than that of 1 mm thick sheets, it remains notably above the lower bound of the targeted response corridor derived from James' equation [18] for PMHS adult skin subjected to spherical or pointed fragments, particularly for the higher 1/SD form factors corresponding to lower SDs. The 0.55 mm 1100-H12 aluminum witness sheet configuration more closely matched the targeted response corridor of the PMHS thigh skin, making it a more suitable alternative to the 2024-T3 alloy as a skin surrogate. However, thin 1100-H12 aluminum sheets are less readily available compared to 2024-T3, which could potentially restrict wider adoption. The analysis of the foam mannequin data indicated that the ballistic resistance of 50 mm-thick panels with a density of 35 kg/m^3 would fall within the response corridor, where the upper bound was defined using James's equation for PMHS adult thigh skin with the coefficient for blunt fragments. EPS and XPS foam materials, being rigid in contrast to soft tissues and gelatin, which are hyperelastic, would not be suitable as a backing material for replicating the as-worn condition. However, a foam panel could replace the 2024-T3 witness sheet for testing fragmentation-resistant body armour material in air-backed conditions when secured onto rigid frames. Polystyrene foam panels would also allow for the soft recovery of target fragments when applying the ballistic limit Protection criterion, as the effect of backing spalling/plugging of the target must then be assessed. Future experimental tests are needed to validate which combination of polystyrene foam grades (EPS or XPS), densities and thicknesses would provide the best response compared to the proposed targeted V_{50} corridor. The ballistic resistance of Al 1100-H12 with lower thicknesses (0.45 and 0.5 mm) should also be characterised over a broad range of sectional densities against projectiles of various shapes (sphere, RCC, FSP) to identify which thickness would better fit the skin perforation targeted corridor. One issue requiring further assessment is the effect on V_{50} of the edge sharpness of non-spherical fragments (FSP, RCC, cubes) [38, 39], which could explain some of the discrepancies in the reported literature. Future research involving PMHS and animal skin samples should evaluate the V_{50} response for lower densities, non-metallic, and smaller fragments, for which the available data are limited. The thickness, body location, and condition (in situ or isolated) of the skin samples used should be well-documented, as they significantly impact perforation resistance. The skin perforation criterion should also be standardised to enhance the repeatability of the results needed for developing improved skin surrogate materials.

References

[1] H. W. Kuhlmann, et al., Interim report on the development of laminated armor, Battelle Memorial Institute, Contract W33-019, Sept 1948, https://apps.dtic.mil/sti/tr/pdf/ADA954855.pdf.
[2] Victory Plastics Co., Ballistic test panels of experimental and standard personal armor materials, Watertown Arsenal Laboratory, File No. WAL 710/1025-3, Dec. 1953, https://apps.dtic.mil/sti/tr/pdf/AD0026368.pdf
[3] Mascianica, F.S., Ballistic Concepts Employed in Testing Lightweight Armor, Watertown Arsenal Laboratory, Monograph Series, Oct 1959, https://apps.dtic.mil/sti/pdfs/AD0609690.pdf
[4] VPAM-PM, Bullet resistant plate materials Requirements, classification, and test procedures, V3-E15, 2021.

https://doi.org/10.52202/081621-0055

[5] US Army, Ballistic tests of armor materials, TOP 2–2–710, Aberdeen Proving Grounds, 1984.
[6] MIL-STD-662F, V50 Ballistic Test for Armor, US Department of Defense standard, Dec 1997.
[7] MIL-STD-3038, Test Methods for Ballistic Defeat Materials, US Department of Defense, May 2011.
[8] National Institute of Justice NIJ, Ballistic Resistant Protective Materials, Standard 0108.01, Sept 1985.
[9] NATO AEP-55, STANAG 4569, Procedures for evaluating the protection level of armoured vehicles -Vol 1: kinetic and artillery threat, NATO Standardization Office (NSO), May 2014.
[10] NATO AEP-97, Multi-Calibre Manual of Proof and Inspection (M-CMOPI) for NATO Small Arms Ammunition, NATO Standardization Office (NSO), October 2020.
[11] US DOD, Purchase Description Enhanced Small Arms Protective Insert (ESAPI), CO/PD 04-19H, 2013.
[12] NATO STANAG 4164, Test Procedures for Armour Perforation Tests of Anti-Armour Ammunition, NATO Standardization Office (NSO), AC/225 D/1375, Nov. 1998.
[13] AEP 2920, (Ed. A, V2), Procedures for the evaluation and classification of personal armour, bullet and fragmentation threats, NATO Standardization Office, Brussels, Sept. 2016.
[14] Frederick, James C., Final Report of Technique and Study of. Witness Materials for Tests Standardization (Ballistic test) (U), Report APG-MT-3187, Tecom Project 9-9-0008-73, Jan. 1969.
[15] Lee, H.C, Meng. H.H., The development of witness plate method for the determination of wounding capability of illegal firearms, January 2011.
[16] Hsiao, Y. T., Meng, H. H., Evaluation of wounding potential of airguns using aluminium witness plates. Australian Journal of Forensic Sciences, 52(4), 2018.
[17] Jakobsen, M.F., An analytical review of perforation statistics – using aluminium as witness plates in perforation experiments, Norwegian Defence Establishment (FFI), FFI Report 23/02387, Dec. 2023.
[18] James G., Development of Models to Assess Penetrating Injury from Ballistic Projectiles, PhD Thesis, Cranfield University, UK, 2020.
[19] McIntosh, G., The Effect of Styrofoam Interlayers in Fragment Witness Packs, DREV-TM-1999-110.
[20] Saw, D., https://euro-sd.com/2025/02/articles/42600/pdws-a-revolution-that-never-quite-happened/
[21] N. Moholkar, Characterising the Ballistic Performance of Polystyrene Foam for the Development of Body Armor Mannequin, DEVCOM, Army Research Lab, Report ARL-CR-0835, Oct 2018.
[22] https://biokinetics.com/product/openbox/
[23] Magnan, S., Pageau, G., et al., "Beyond V50, A More Comprehensive and Efficient Methodology for Assessing Armour Performance", Proc. PASS-2023, Dresden, Germany, 2023,
[24] IDA, Binary data logistic regression, https://test-science.shinyapps.io/LogisticRegression/
[25] Hudgins, H., 2005. Estimating ballistic limits of skin and clothing for projectiles, 40th Annual Armament Systems: Guns - Ammunition - Rockets - Missiles (GARM).
[26] Y. Baillargeon, C. Lalanne, Hole Growth Equation Related to Al-1100 Witness Plates, Defence R&D Canada, Report DRDC-TM-2003-122, August 2004.
[27] D. Bourget, Y. Baillargeon, S. Northrop, Witness Pack Calibration for Human Vulnerability Assessment, Proc. 20th Int. Symposium on Ballistics, Orlando, Florida, US, Sept. 2002.
[28] Verolme, J.L., M. Szymczak, and J. Broos, Metallic witness packs for behind-armour debris characterisation, International Journal of Impact Engineering, Volume 22, Issue 7, August 1999.
[29] Nguyen TN, Tsukada H, James GR, et al, Experimental model and simulant for studying blast penetrating injury to the skin, J Mech Behav Biomed Mater, May 2025.
[30] LeSueur J, Koser J, Hampton C, Kleinberger M, Pintar FA. Penetration Thresholds of Porcine Limbs for Low Sectional Density Projectiles in High-Rate Impact. Mil Med. 2024 Aug 19;189(Suppl 3).
[31] Cunniff P., Variability in ballistic impact performance due to projectile physical properties and dimensions, Proc. 24th Int. Symp. on Ballistics, New Orleans, LA, Sept 2008.
[32] Pandey, P.K., et al, Review of Interaction of Bullets and Fragments With Skin-Bone-Muscle Parenchyma, ASME J of Medical Diagnostic, Paper No: JESMDT-24-1044, Nov 2025.
[33] Bir, C. A., Stewart, S. J., & Wilhelm, M., Skin Penetration Assessment of Less Lethal Kinetic Energy Munitions, Journal of Forensic Sciences, 50(6), 2005.
[34] Foley, S. et al., Evaluation of Skin Penetration from Less Lethal Impact Munitions, 33rd Int. Symp. on Ballistics, 2023, Bruges, Belgium, https://ibrc.osu.edu/wp-content/uploads/2023/05/Foley-IBS-Paper.pdf
[35] Shedd, D., et al., The risk of skin injury caused by high-rate blunt impacts to the human thorax. Human Factors and Mechanical Engineering for Defense and Safety, Vol. 6, No. 5, 2022.
[36] Hyams, D.G., 2021, https://curveexpert-professional.software.informer.com/1.6/
[37] Kokinakis W, Sperrazza J., Criteria for incapacitating soldiers with fragments and flechettes, Ballistic Res Lab 1965, Available at https://apps.dtic.mil/sti/citations/AD0359774.
[38] Cline J., et al., The ballistic response of woven Kevlar fabric as a function of projectile sharpness, US Army Research Laboratory Report ARL-TR-8694, May 2019.
[39] F. Barbillon, et al., review of fragment simulating projectiles definition and associated quality controls needed, Proc. PASS-2020, Copenhagen, Denmark, October 2021.